MATHEMATICAL MODELING AND COMPUTING, Vol. 12, No. 3, pp. 936–949 (2025)

# Hybrid trigonometric Bézier interpolation with uniform, chordal and centripetal parameterization in 3-Euclidean space and its application

Mohamed D., Ramli A. L. A.

*School of Mathematical Sciences, University Sains Malaysia (USM), 11800 Pulau Pinang, Malaysia*

(Received 19 February 2025; Revised 2 September 2025; Accepted 9 September 2025)

Interpolation in trigonometric Bézier curves refers to constructing a curve that smoothly passes through a given set of control points. In this paper, data points are interpolated by the General Hybrid Trigonometric Bézier (GHTB) curve. The curve contains four free parameters that allow flexibility in curve construction. The determination of control points on the GHTB curve, based on a certain degree, results in the interpolation of the curve that passes through the data points. Uniform, centripetal, and chordal parameterization methods are applied to GHTB curves. The three parametrization techniques — uniform, centripetal, and chordal — of the GHTB curve are discussed. Subsequently, the demonstration of these parametrization methods is carried out using sets of data points in both 2-dimensional and 3-dimensional Euclidean space. The curvatures and torsion of the parametrized curves for various values of free parameters in the GHTB curve are observed.

**Keywords:** *general hybrid trigonometric Bézier curve; uniform parametrization; centripetal parametrization; chordal parametrization; curvature; torsion.*

**2010 MSC:** 65D17, 65D10 **DOI:** 10.23939/mmc2025.03.936

## 1. Introduction

Modifying the control points of a regular Bézier curve to achieve a desired form, while ensuring that the curve passes specific points or adheres to certain constraints, is known as the interpolation of geometric Bézier curves using shape parameters. Interpolation may be accomplished through various methods, with the most common ones being linear interpolation, polynomial interpolation (utilizing polynomials of varying degrees) [1], and spline interpolation (using piecewise-defined polynomials of higher degrees) [2]. These techniques aim to find the curve with the least overall error or variation in the data.

Curve interpolation finds applications in various fields such as computing, statistics, image processing, and user interface design. It enables the seamless generation of data approximations for visualization, modeling, and prediction. The Bernstein–Bézier curve technique was investigated for data interpolation whereby the curves fulfill the aesthetic substance requirements [3]. Pythagorean hodograph (PH) curves of degree five were proposed for Hermite interpolation, and the $C^1$ four Hermite border was applied for a PH quintic structure interpolating Hermite [4]. The presence of zero, one, or two distinct solutions for $G^1$ Hermite interpolation using PH cubic segments [5] is contingent upon the orientation of the end tangent $t_1$ and $t_2$ concerning the endpoint displacement vector $\Delta p = p_1 - p_0$. A method for $G^1$ interpolation with a single Cornu spiral segment was proposed such that a smoothly fitting curve can be generated between two locations with tangent directions but not curvatures [6]. A geometric approach for interpolating a sequence of data points, unit tangential, and curvature vectors was developed using a uniform cubic B-spline curve [7]. A novel cubic Hermite trigonometric spline interpolation method was designed for curves and surfaces with form parameters [8]. Discrete logarithmic spirals were used to interpolate $G^1$ curves [9]. A quintic Bézier curve was used for planar $G^3$ Hermite

This research is supported by the Ministry of Higher Education Malaysia through Fundamental Research Grant Scheme (FRGS/1/2021/STG06/USM/02/6).

 

interpolation [10]. An improved version of the centripetal parameterization method for B-spline data interpolation was proposed [11]. On the other hand, a particular road curve was reconstructed by using Bézier curve fitting on a map with the aid of various parameterization approaches [12]. A new method for interpolating a cubic B-spline curve was demonstrated by considering the first and second derivatives at endpoints and only the first derivative at inner points [13].

Bézier curves are used in computer graphics, CAD, and other industries to generate smooth, curved objects. Control points and Bernstein basis functions can be used to create traditional Bézier curves. It is possible to build diverse forms utilizing parametric or geometric continuity to satisfy our design needs after building the necessary Bézier curves and surfaces [1]. Various Bézier curves and surfaces with shape parameters could be explored, each of which has more properties than the original [14]. Shape design is a time-consuming procedure. A design usually cannot be completed in a single phase even after applying continuity criteria. To get around this difficult situation, two distinct functions are defined to create these curves and surfaces in tuples of two and three. The form parameters of the trigonometric Bézier curve were considered because they are more continuous than the polynomial Bézier curve [15, 16]. Bibi et al. [17] had already created diverse curve shapes and typeface designs while also defining the curvature of generalized hybrid trigonometric Bézier (GHT-Bézier) curves by incorporating parametric and geometric continuity constraints. The presentation includes a demonstration of generalized hybrid trigonometric Bernstein (GHT-Bernstein) basis functions and Bézier curves featuring shape parameters. A new class of generalized trigonometric Bernstein-like bases of $k$-th degree (referred to as GT-Bernstein) was also introduced. The newly developed basis function, which includes two shape parameters, shares similarities with the Bernstein basis functions [18]. In a clear formulation, a novel recursive formula was devised to generate the polynomial functions of degree $m$, known as the generalized blended trigonometric Bernstein (GBT-Bernstein) [19]. Using these basis functions, this paper establishes generalized blended trigonometric Bézier (GBT-Bézier) curves incorporating two form parameters. The study delves into exploring the geometric characteristics of these curves and investigates their applications in curve modeling.

Beyond maintaining the shapes of curves and surfaces, the Bernstein basis functions introduced here also convey several geometric properties not observed in the standard Bernstein basis functions of the past. These fundamental functions are crucial for defining and analysing the geometric features of generalized trigonometric Bézier (GT-Bézier) curves and surfaces, which can be compared to classical Bézier curves and surfaces. A novel rational quadratic, trigonometric Bézier curve was introduced by Bashir et al. [20], comparable to the conventional rational quadratic Bézier curve. The existence of shape parameters grants the designer a sense of intuitive manipulation over the form of the curve. To address the limitation of traditional Bézier curves in generating complex curves, Usman et al. [21] developed trigonometric cubic Bézier-like curves with single-shape parameters. Furthermore, a novel sextic trigonometric-Bernstein basis and Bézier curve, incorporating two shape parameters, was introduced [22]. A proposed curve can be utilized to generate both open and closed curves with varying values of form parameters. For instance, five templates for spiral transition curves that utilize cubic GHT-Bézier equations were presented [23]. A novel technique that generates a seamless trajectory (devoid of impediments) using cubic GHT-Bézier spiral curves was introduced. The shortest distance, bending energy, and curvature variation energy were minimized to provide a smooth path without obstacles. To tackle the problem of modeling and creating surfaces, continuity constraints were introduced between two generalized Bézier-like surfaces (gBS) with distinct shape characteristics [24].

This paper introduces the interpolation of the GHT-Bézier curve. By using the concept of the three parametrization methods namely uniform, centripetal, and chordal, the cubic hybrid trigonometric Bézier (CHTB) curve interpolated a given data sets. The motivation of this work is to investigate parameterization within the context of trigonometric Bézier curves. Unlike the parameterization of integral Bézier curves, which lacks free parameters for shape adjustment [12], trigonometric Bézier curves offer greater flexibility in their construction. Therefore, it is important to explore how parameterized curves can be constructed and utilized in this framework.

Moreover, the concepts of curvature and torsion are introduced for a space curve. Torsion quantifies the rotational displacement of a space curve from the plane of curvature as it advances along its longitudinal axis. Curvature quantifies the degree of sharpness with which a curve forms a bend at a specific location. The fundamental principles are implemented on the interpolated CHTB space curve to highlight our methodology. This paper focuses on the effect of interpolation by using the introduced parametrization methods on the CHTB curve in two-dimensional (2D) and three-dimensional (3D) Euclidean spaces through simple modeling figures and shape parameters' effect on the interpolated curve.

## 2. Preliminary concepts

This section will introduce basic information about a GHTB curve and its properties. Reference [25] proposed an important idea to address challenges in constructing symmetric revolutionary curves and rotation surfaces in engineering. The GHT-Bézier curve is utilized for this purpose. The alteration of shape parameters enables the modification of the curves and surfaces. Free-form complex curves are constructed by employing GHT-Bézier curves with constraints of parametric continuity.

**Definition 1 (Ref. [25]).** *For $n=2$, the quadratic hybrid trigonometric (QHT) Bernstein basis functions in terms of variable $u \in [0,1]$ are defined as follows:*

$$q_{0,2}(u) = \left(1-\sin\tfrac{\pi u}{2}\right)\left[\left(1-\nu\sin\tfrac{\pi u}{2}\right)e^{\gamma u} + \lambda\left(1-\cos\tfrac{\pi u}{2}\right)\right], \tag{1}$$

$$q_{2,2}(u) = \left(1-\cos\tfrac{\pi u}{2}\right)\left[\left(1-\beta\cos\tfrac{\pi u}{2}\right)e^{\gamma(1-u)} - \lambda\left(1-\sin\tfrac{\pi u}{2}\right)\right], \tag{2}$$

$$q_{1,2}(u) = 1 - q_{0,2}(u) - q_{2,2}(u), \tag{3}$$

*and are known as GHT-Bernstein basis functions. The function $q_{i,n}(u)=0$ if and only if $i=-1$ or $i>n$. The variables $\nu,\beta,\gamma \in [-1,1]$ and $\lambda \in [-1.5, 0.5]$ are the shape parameters defined in the given domain. These functions satisfy some properties such as non-negativity, partition of unity, symmetry, and terminals property of the curve.*

**Definition 2 (Ref. [20]).** *A class of parametric GHT-Bézier curves with a given set of control points $P_i$ $(i=0,1,2,3,\dots,n)$ and shape parameters $\nu,\beta$, and $\gamma$ are defined by the following equation:*

$$S(u,\beta,\nu,\gamma,\lambda) = \sum_{i=0}^{n} P_i q_{i,n}(n), \quad 0 \leqslant u \leqslant 1, \tag{4}$$

*where $q_{i,n}(n)$ are the GHT-Bernstein basis functions and variables $\beta,\nu,\gamma$, and $\lambda$ are the shape parameters.*

By assuming that every curve can be drawn using the Cartesian coordinate system in $\mathbb{E}^3$, the control points are viewed as a pair of tuples [1],

$$v(t) = (v_x, v_y, v_z), \quad u(t) = (u_x, u_y, u_z), \tag{5}$$

and the Euclidean norm of a vector a can be defined as

$$\|v\| = \sqrt{v_x^2 + v_y^2 + v_z^2}, \quad \|u\| = \sqrt{u_x^2 + u_y^2 + u_z^2}. \tag{6}$$

The inner and cross products of the two curves are

$$\langle v(t), u(t)\rangle = \sqrt{v_x \cdot u_x + v_y \cdot u_y + v_z \cdot u_z}, \tag{7}$$

$$v(t) \times u(t) = (v_y u_z - u_y v_z)e_1 - (v_x u_z - u_x v_z)e_2 + (v_x u_y - u_x v_y)e_3. \tag{8}$$

The curvature and torsion of the parametric curve $u(t) = (u_x, u_y, u_z)$ are given by

$$\kappa(t) = \frac{\|u'(t) \times u''(t)\|}{\|u'(t)\|^3}, \tag{9}$$

$$\tau(t) = \frac{\mathrm{Det}[u'(t), u''(t), u'''(t)]}{\|u'(t) \times u''(t)\|^2}. \tag{10}$$

The functions $u'(t)$, $u''(t)$, and $u'''(t)$ represent the first, the second, and the third derivative of $u(t)$ sequentially.

## 3. Methodology

### 3.1. Parametrization methods

Researchers employed various parametrization techniques. Given the absence of discussion on the parametrization approach in relation to the trigonometric Bézier curve, this work specifically examines three distinct types of parameterizations: uniform, chordal, and centripetal.

**Uniform parametrization.** Calculating the parameter values is the simplest method available. This method is recommended if the target datasets are evenly distributed. According to the assumption that the parameters are normalized, this range is divided into $n$ pieces linearly if there are $n+1$ data points. $t_0$ is zero, while $t_n$ is one. Other variables are calculated as follows:

$$t_i = \frac{i}{n}, \quad 1 \leqslant i \leqslant n-1. \tag{11}$$

The computation of uniform parameterization is fundamentally straightforward. However, employing this approach may lead to unintended consequences. Where the data distribution is uneven, such as in a non-uniform distribution of parameters, the parameterization technique may lead to wobbles. Several alternative approaches had been developed to address this problem, and a comprehensive plan had been formulated.

**Chordal parametrization method.** This method was used by Saffie and Ramli [12] for the Bézier curve. Assume data points are $(Q_0, Q_1, Q_2, \ldots, Q_n)$. The power factor is $\alpha = 1$. The distance between two adjacent data points is defined as $|Q_i - Q_{i-1}|$. In this case, the length of the data polygon is

$$L = \sum_{i=1}^{k} |Q_i - Q_{i-1}|. \tag{12}$$

The initial and final parameters are specified as $t_0 = 0$ and $t_n = 1$. The middle parameters are distributed in the range of $(0,1)$ according to the following equation:

$$t_k = \frac{1}{L} \sum_{i=1}^{k} |Q_i - Q_{i-1}|. \tag{13}$$

**Centripetal parametrization method.** This method was also used by Saffie and Ramli [12]. Using the same data points $(Q_0, Q_1, Q_2, \ldots, Q_n)$ and the power factor is taken as $\alpha = 0.5$, the distance between two adjacent data points is defined by $|Q_i - Q_{i-1}|^\alpha$. In this case, the length of the data polygon is

$$L = \sum_{i=1}^{k} |Q_i - Q_{i-1}|^\alpha. \tag{14}$$

Similarly, the initial and final parameters are specified as $t_0 = 0$ and $t_n = 1$. The middle parameters are distributed in the range of $(0,1)$ according to the following equation:

$$t_k = \frac{1}{L} \sum_{i=1}^{k} |Q_i - Q_{i-1}|^\alpha. \tag{15}$$

### 3.2. Interpolating of general hybrid trigonometric Bézier curve

In this section, the interpolation methods of the GHT-Bézier curve at different values of shapes of control points will be investigated. When the data points are interpolated, it is assumed that the data is not noisy (i.e., it does not contain errors). Usually, the user will define its control points to construct the GHT-Bézier curve. In this paper, the data points are given instead of control points, and the generated GHT-Bézier curves must pass through a set of control points, $b_m \in \mathbb{R}^d$ $(m = 0, 1, \ldots, k;\ d = 2, 3)$ that needs to be determined. The GHT-Bernstein basis functions $I_{m,k}(t)$ and shape parameters $\nu, \gamma, \beta, \lambda$ form the following equations:

$$I_{0,2}(t) = \left(1 - \sin\tfrac{\pi t}{2}\right)\left(1 - \nu \sin\tfrac{\pi t}{2}\right) e^{\gamma u} + \lambda\left(1 - \cos\tfrac{\pi t}{2}\right), \tag{13}$$

$$I_{1,2}(t) = 1 - I_{0,2}(t) - I_{2,2}(t), \tag{16}$$

$$I_{2,2}(t) = \left(1 - \cos\tfrac{\pi t}{2}\right)\left(1 - \beta\cos\tfrac{\pi t}{2}\right)e^{\gamma(1-t)} - \lambda\left(1 - \sin\tfrac{\pi t}{2}\right), \tag{17}$$

$$I_{m,k}(t) = (1-t)I_{m,k-1}(t) + t\,I_{m-1,k-1}(t). \tag{18}$$

The parametric GHT-Bézier curves with the given set of control points $b_m$ is given by

$$H(t;\gamma,\beta,\lambda,\nu) = \sum_{m=0}^{k}(1-t)\,I_{m,k-1}(t)\,b_m + \sum_{m=0}^{k} t\,I_{m-1,k-1}(t)\,b_m, \quad 0 \leqslant t \leqslant 1. \tag{19}$$

Consider a set of points $Q_j = (x_j, y_j)$, such that $0 \leqslant j \leqslant n$, obtained as structured data points. Assuming that no two consecutive points $Q_j$ are the same, consider the problem of interpolating a trigonometric Bézier curve through these data points such that

$$H(t_j,\gamma,\beta,\lambda,\nu) = Q_j = (x_j, y_j), \quad \text{where } t_0 \leqslant t_1 \leqslant \ldots \leqslant t_n. \tag{20}$$

Certain chosen parameter values called interpolating nodes can expand Eq. (15) as follows:

$$H(t_0,\gamma,\beta,\lambda,\nu) = Q_0; \quad \sum_{m=0}^{k}(1-t_0)\,I_{m,k-1}(t_0)\,b_m + \sum_{m=0}^{k} t_0\,I_{m-1,k-1}(t_0)\,b_m = Q_0, \tag{21}$$

$$H(t_1,\gamma,\beta,\lambda,\nu) = Q_1; \quad \sum_{m=0}^{k}(1-t_1)\,I_{m,k-1}(t_1)\,b_m + \sum_{m=0}^{k} t_1\,I_{m-1,k-1}(t_1)\,b_m = Q_1, \tag{22}$$

$$H(t_2,\gamma,\beta,\lambda,\nu) = Q_2; \quad \sum_{m=0}^{k}(1-t_2)\,I_{m,k-1}(t_2)\,b_m + \sum_{m=0}^{k} t_2\,I_{m-1,k-1}(t_2)\,b_m = Q_2, \tag{23}$$

$$\vdots \tag{24}$$

$$H(t_n,\gamma,\beta,\lambda,\nu) = Q_n; \quad \sum_{m=0}^{k}(1-t_n)\,I_{m,k-1}(t_n)\,b_m + \sum_{m=0}^{k} t_n\,I_{m-1,k-1}(t_n)\,b_m = Q_n. \tag{25}$$

The end interpolating points at $t_0 = 0$ and $t_n = 1$ are as follows:

$$I_{0,k-1}(0)\,b_0 + \sum_{m=1}^{k} I_{m-1,k-1}(0)\,b_m = Q_0, \tag{26}$$

$$I_{k-1,k-1}(1)\,b_k + \sum_{m=0}^{k} I_{m-1,k-1}(1)\,b_m = Q_n. \tag{27}$$

Substituting Eq. (17) into Eq. (16) yields

$$\sum_{m=0}^{k}(1-t_1)\,I_{m,k-1}(t_1)\,b_m + \sum_{m=0}^{k} t_1\,I_{m-1,k-1}(t_1)\,b_m = Q_1, \tag{28}$$

$$\begin{aligned}\sum_{m=1}^{k-1}\left((1-t_1)\,I_{m,k-1}(t_1) + t_1\,I_{m-1,k-1}(t_1)\right)b_m = Q_1 &- \left[(1-t_1)\,I_{0,k-1}(t_1) + t_1\,I_{0-1,k-1}(t_1)\right]b_0 \\ &- \left[(1-t_1)\,I_{k,k-1}(t_1) + t_1\,I_{k-1,k-1}(t_1)\right]b_k.\end{aligned} \tag{29}$$

Similarly, at the second data point, expanding the other formula at $m = 0$ and $m = k$ gives

$$\sum_{m=0}^{k}(1-t_2)\,I_{m,k-1}(t_2)\,b_m + \sum_{m=0}^{k} t_2\,I_{m-1,k-1}(t_2)\,b_m = Q_2, \tag{30}$$

$$\begin{aligned}\sum_{m=1}^{k-1}\left((1-t_2)\,I_{m,k-1}(t_2) + t_2\,I_{m-1,k-1}(t_2)\right)b_m = Q_2 &- \left[(1-t_2)\,I_{0,k-1}(t_2) + t_2 I_{0-1,k-1}(t_2)\right]b_0 \\ &- \left[(1-t_2)\,I_{k,k-1}(t_2) + t_2\,I_{k-1,k-1}(t_2)\right]b_k.\end{aligned} \tag{31}$$

Formulation for the generalized $n$ can be obtained by expanding the next formula at $m = 0$ and $m = k$, resulting in

$$\begin{aligned}
&\sum_{m=0}^{k}(1-t_{n-1})\,I_{m,k-1}(t_{n-1})\,b_m + \sum_{m=0}^{k} t_{n-1}\,I_{m-1,k-1}(t_{n-1})\,b_m = Q_{n-1},\\
&\sum_{m=1}^{k-1}\left((1-t_{n-1})\,I_{m,k-1}(t_{n-1}) + t_{n-1}\,I_{m-1,k-1}(t_{n-1})\right)b_m = Q_{n-1}\\
&\quad - \left[(1-t_{n-1})\,I_{0,k-1}(t_{n-1}) + t_{n-1}\,I_{0-1,k-1}(t_{n-1})\right]b_0\\
&\quad - \left[(1-t_{n-1})\,I_{k,k-1}(t_{n-1}) + t_{n-1}\,I_{k-1,k-1}(t_{n-1})\right]b_k.
\end{aligned} \tag{32}$$

In order to solve the system of equations for the control points $b_1, b_2, \ldots, b_{k-1}$, the system above can be converted into the matrix form $A \cdot B = M$, where

$$A = \begin{pmatrix} a_{1,1} & a_{1,2} & \cdots & a_{1,k-1} \\ a_{2,1} & a_{2,2} & \cdots & a_{2,k-1} \\ \vdots & \vdots & \ddots & \vdots \\ a_{n,1} & a_{n,2} & \cdots & a_{n,k-1} \end{pmatrix},$$

$$\begin{aligned}
a_{1,1} &= (1-t_1)I_{1,k-1}(t_1) + t_1 I_{0,k-1}(t_1),\\
a_{1,2} &= (1-t_1)I_{2,k-1}(t_1) + t_1 I_{1,k-1}(t_1),\\
&\vdots\\
a_{1,k-1} &= (1-t_1)I_{k-1,k-1}(t_1) + t_1 I_{k-2,k-1}(t_1), \qquad (33)\\
a_{2,1} &= (1-t_2)I_{1,k-1}(t_2) + t_2 I_{0,k-1}(t_2),\\
a_{2,2} &= (1-t_2)I_{2,k-1}(t_2) + t_2 I_{1,k-1}(t_2),\\
&\vdots\\
a_{2,k-1} &= (1-t_2)I_{k-1,k-1}(t_2) + t_2 I_{k-2,k-1}(t_2), \qquad (34)\\
a_{n,1} &= (1-t_n)I_{1,k-1}(t_n) + t_n I_{0,k-1}(t_n),\\
a_{n,2} &= (1-t_n)I_{2,k-1}(t_n) + t_2 I_{1,k-1}(t_n),\\
&\vdots\\
a_{n,k-1} &= (1-t_n)I_{k-1,k-1}(t_n) + t_2 I_{k-2,k-1}(t_n), \qquad (35)
\end{aligned}$$

$$A = \begin{pmatrix} a_{1,1} & a_{1,2} & \cdots & a_{1,k-1} \\ a_{2,1} & a_{2,2} & \cdots & a_{2,k-1} \\ \vdots & \vdots & \ddots & \vdots \\ a_{n,1} & a_{n,2} & \cdots & a_{n,k-1} \end{pmatrix},$$

$$B = \begin{pmatrix} b_1 \\ b_2 \\ \vdots \\ b_{k-1} \end{pmatrix},$$

and the matrix $M$ can be defined as

$$\begin{pmatrix}
Q_1 - [(1-t_1)I_{0,k-1}(t_1) + t_1 I_{0-1,k-1}(t_1)] - [(1-t_1)I_{k,k-1}(t_1) + t_1 I_{k-1,k-1}(t_1)] \\
Q_2 - [(1-t_2)I_{0,k-1}(t_2) + t_2 I_{0-1,k-1}(t_2)] - [(1-t_2)I_{k,k-1}(t_2) + t_2 I_{k-1,k-1}(t_2)] \\
\vdots \\
Q_{n-1} - [(1-t_{n-1})I_{0,k-1}(t_{n-1}) + t_{n-1} I_{0-1,k-1}(t_{n-1})] \\
- [(1-t_{n-1})I_{k,k-1}(t_{n-1}) + t_{n-1} I_{k-1,k-1}(t_{n-1})]
\end{pmatrix}.$$

The matrix $B$ can be obtained by

$$\begin{pmatrix} b_1 \\ b_2 \\ \vdots \\ b_{k-1} \end{pmatrix} = A^{-1} \cdot M.$$

## 4. Results

### 4.1. Parametrization of cubic-general hybrid trigonometric Bézier curve in $\mathbb{E}^2$

The uniform parametrization can then be implemented for Eq. (1). This method is recommended if the target datasets are evenly distributed. Consider CHTB curve with control points $b_0$, $b_1$, $b_2$, $b_3$, and shape parameters $\nu$, $\beta$, $\gamma$, and $\lambda = 0$. For demonstration purposes, the data points are chosen as the following:

$$Q_0 = (0, \pi/2), \quad Q_1 = (\pi, 3\pi/2), \quad Q_2 = (2\pi, 5\pi/3), \quad Q_3 = (10, 3). \tag{28}$$

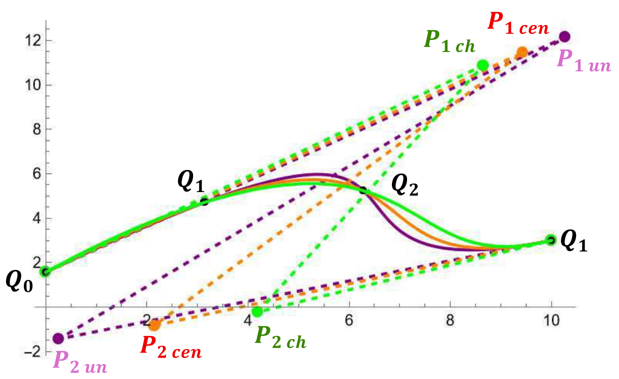


**Fig. 1.** Uniform, chordal, and centripetal parametrization of CHTB curves at shape parameters $\beta = 1$, $\nu = -1$, $\gamma = 1$, and $\lambda = 0$.

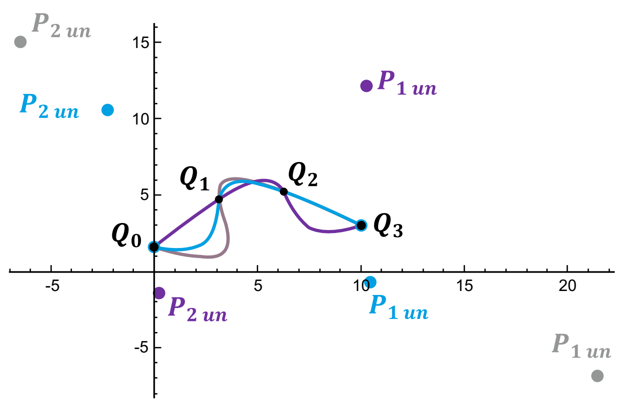


**Fig. 2.** Uniform parametrization of CHTB curves at shape parameters $\beta = (-1, 1)$, $\nu = (-1, -0.5, 0, 1)$, $\gamma = 1$, and $\lambda = 0$.

Figure 1 shows the comparison of uniform, chordal, and centripetal parametrization of CHTB curves at shape parameters $\beta = 1$, $\nu = -1$, $\gamma = 1$, and $\lambda = 0$. For design purposes, a specific curve cannot be pointed to as better than the others. It is only noted that the chordal parametrization is less curvy compared to centripetal and uniform parameterization. The control points of these curves vary depending on the parametrization.

Figure 2 shows the uniform parametrized CHTB curves with different values of shape parameters on the same data points. Both figures use the shape parameters $\gamma = 1$ and $\lambda = 0$. As the other shape parameters $\beta$ and $\nu$ are changed, the curve will also change its shape while maintaining the interpolation on the data points. The control points of the curve are also different as shape parameters vary.

Figure 3 shows the curvatures of uniform parametrized CHTB curves. The values of curvature shown are absolute values. The curvatures for purple and cyan curves with the shape parameters $\beta = 0$, $\nu = 0$ and 1 respectively, $\gamma = 1$, and $\lambda = 0$ are twisted smoothly.

Figure 4 shows the chordal parametrization of CHTB curves and the effect of different shape parameters using the same shape parameters and data points in Figure 2. In chordal parametrization, the smoothness of the parametrized CHTB curves between the $Q_1$ and $Q_2$ movements are more apparent than uniform parameterization.

Figure 5 displays the curvatures of the curves presented in Figure 4. The curvature values are lower than the uniform counterpart, indicating that the curve is relatively less curvy.

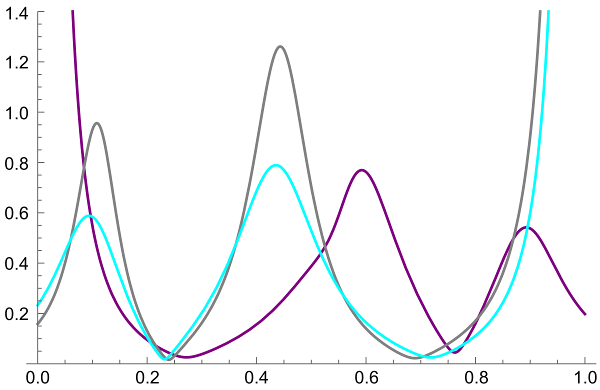

**Fig. 3.** Curvatures of uniform parametrization of CHTB curves at shape parameters $\beta = (-1, 1)$, $\nu = (-1, -0.5, 0, 1)$, $\gamma = 1$, and $\lambda = 0$.

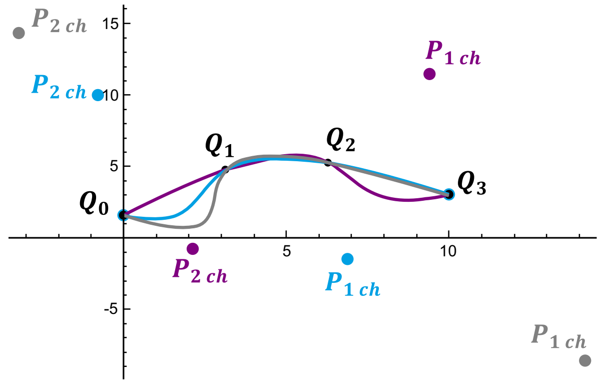


**Fig. 4.** Chordal parametrization of CHTB curves at shape parameters $\beta = (-1, 1)$, $\nu = (-1, -0.5, 0, 1)$, $\gamma = 1$, and $\lambda = 0$.

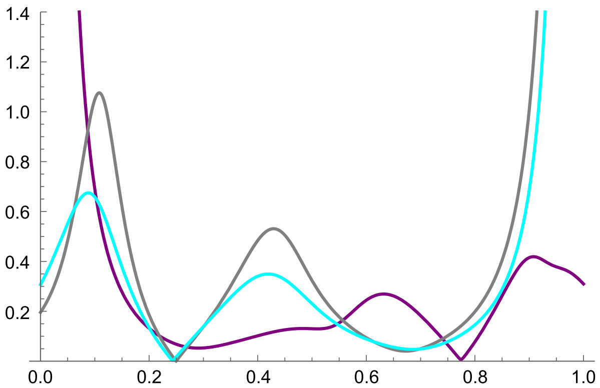

**Fig. 5.** Curvatures of chordal parametrized CHTB curves at shape parameters $\beta = (-1, 1)$, $\nu = (-1, -0.5, 0, 1)$, $\gamma = 1$, and $\lambda = 0$.

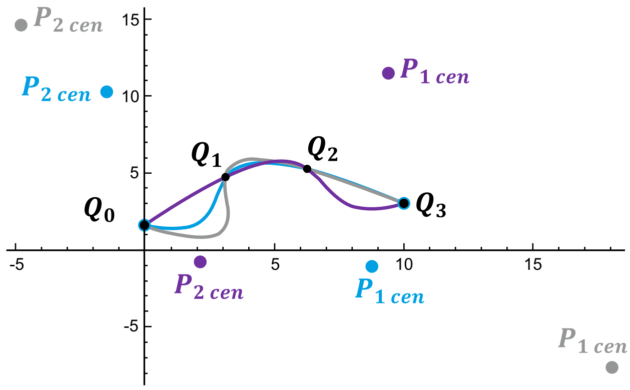


**Fig. 6.** Centripetal parametrization of CHTB curves at shape parameters $\beta = (-1, 1)$, $\nu = (-1, -0.5, 0, 1)$, $\gamma = 1$ and $\lambda = 0$.

The centripetal parametrization of CHTB curves and their curvatures at $\beta = (-1, 1)$, $\nu = \{-1, -0.5, 0, 1\}$, $\gamma = 1$, and $\lambda = 0$ are displayed in Figures 6 and 7, respectively. Visually, the centripetal parametrization resembles the chordal parameterization.

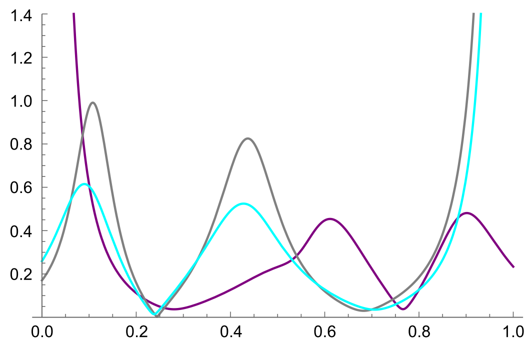

**Fig. 7.** Curvatures of centripetal parametrized CHTB curves at shape parameters $\beta = (-1, 1)$, $\nu = (-1, -0.5, 0, 1)$, $\gamma = 1$, and $\lambda = 0$.

### 4.2. Parametrization of cubic-general hybrid trigonometric Bézier curve in $\mathbb{E}^3$

In this section, the CHTB curve interpolation in 3D space is demonstrated. The following data points are considered:

$$Q_0 = \left(0, \frac{\pi}{2}, 1\right),$$
$$Q_1 = \left(\pi, \frac{3\pi}{2}, \frac{\pi}{2}\right),$$
$$Q_2 = \left(2\pi, \frac{5\pi}{3}, \frac{3\pi}{2}\right),$$
$$Q_3 = (10, 3, 1).$$

Figures 8 and 9 illustrate the movements of uniform parametrized CHTB curves. Figure 8 depicts the red curve with shape parameters $\beta = -1$, $\nu = 1$, $\gamma = 1$, and $\lambda = 0$, while the grey curve is generated using parameters $\beta = -1$ and $\nu = 0$. The shape of the curve is adjustable and varies based on its parameters.

The properties of the curve can be assessed by analysing its curvature and torsion. Figure 9 demonstrates the curvature of the red and grey curves. The grey curve exhibits a higher curvature as it bends more compared to the red curve. Figure 10 illustrates the torsion of both curves. The red curve has a slightly higher torsion, indicating that it twists more than the grey curve.

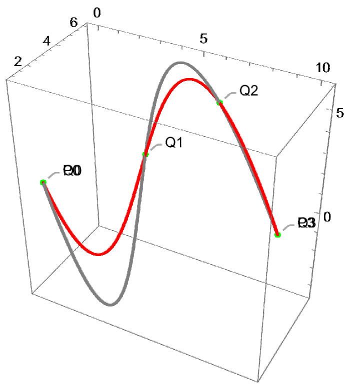


**Fig. 8.** Uniform parametrization of CHTB curves at shape parameters $\beta = -1$, $\nu = (1, 0.5)$, $\gamma = 1$, and $\lambda = 0$.

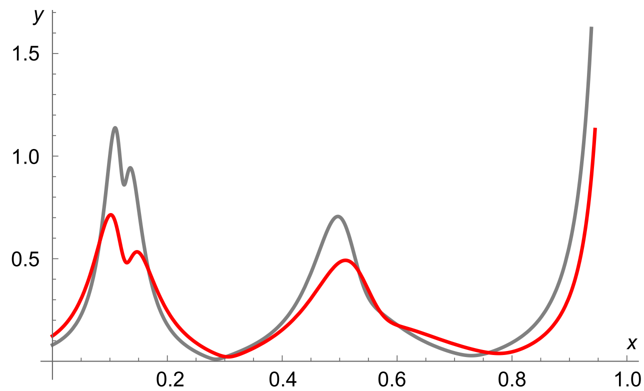


**Fig. 9.** Curvatures of uniform parametrization of CHTB curves at shape parameters $\beta = -1$, $\nu = (1, 0.5)$, $\gamma = 1$, and $\lambda = 0$.

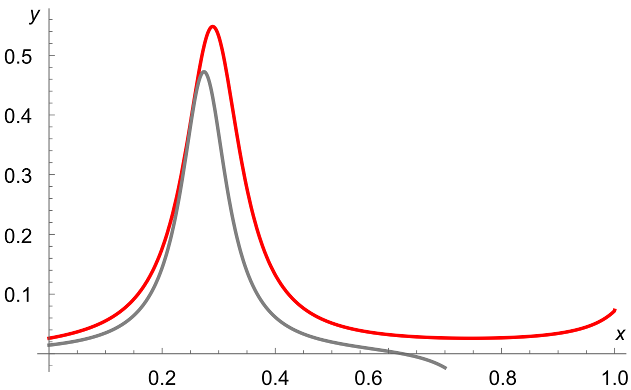


**Fig. 10.** Torsions of uniform parametrization of CHTB curves at shape parameters $\beta = -1$, $\nu = (1, 0.5)$, $\gamma = 1$, and $\lambda = 0$.

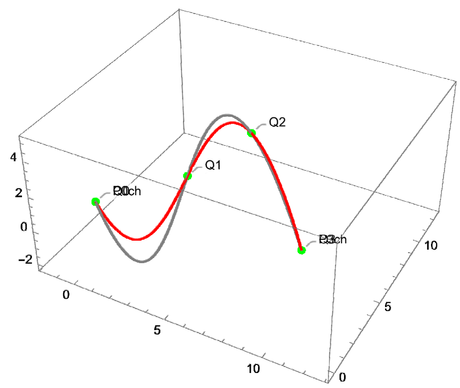


**Fig. 11.** Chordal parametrization of CHTB curves at shape parameters $\beta = -1$, $\nu = (1, 0.5)$, $\gamma = 1$, and $\lambda = 0$.

Using similar data points and shape parameters, Figures 11, 12, and 13 present the chordal parametrization CHTB curves, corresponding curvatures, and corresponding torsions, respectively. Figures 14, 15, and 16 display the centripetal parametrization counterparts.

By comparing the grey curve in Figures 11 and 14, the grey centripetal curve is observed to be slightly different from the chordal one. Furthermore, the curvature of the centripetal grey curve exhibits a high peak, indicating that it is highly twisty. The torsion of the centripetal grey curve is observed to be more twisted than the

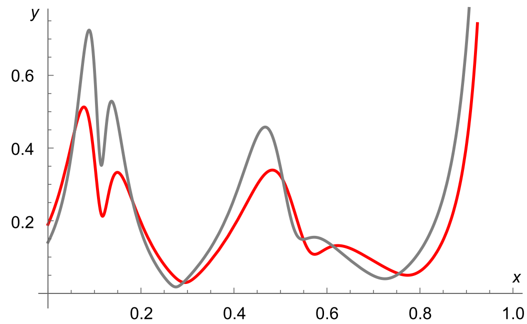


**Fig. 12.** Curvatures of chordal parametrization of CHTB curves at shape parameters $\beta = (-1, 0)$, $\nu = (1, 0.5)$, $\gamma = 1$, and $\lambda = 0$.

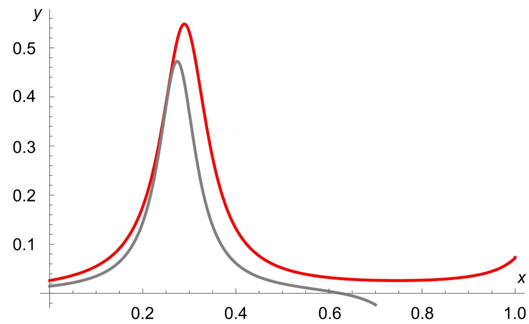


**Fig. 13.** Torsions of chordal parametrization of CHTB curves at shape parameters $\beta = -1$, $\nu = (1, 0.5)$, $\gamma = 1$, and $\lambda = 0$.

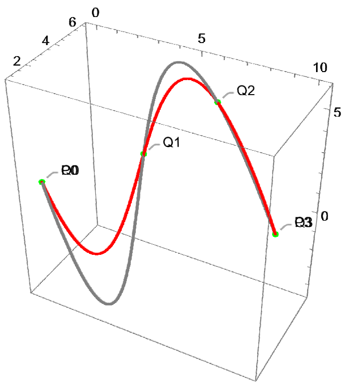


**Fig. 14.** Centripetal parametrization of CHTB curves at shape parameters $\beta = (1, 0)$, $\nu = 1$, $\gamma = 1$, and $\lambda = 0$.

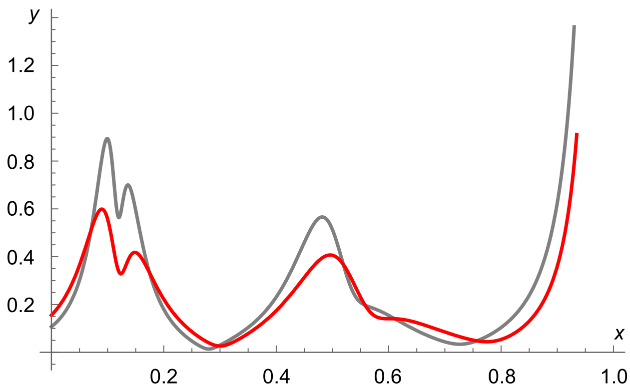


**Fig. 15.** Curvatures of centripetal parametrization of CHTB curves at shape parameters $\beta = (1, 0)$, $\nu = 1$, $\gamma = 1$, and $\lambda = 0$.

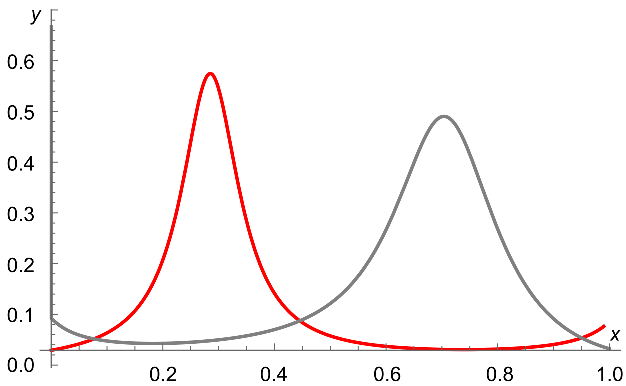


**Fig. 16.** Torsions of centripetal parametrization of CHTB curves at shape parameters $\beta = (1, 0)$, $\nu = 1$, $\gamma = 1$, and $\lambda = 0$.

### 4.3. Curve generation with user-defined points

In this section, it is demonstrated how a curve can be drawn by defining points instead of control points. The flower drawings in Figure 17$a$ illustrate the behavior of interpolated curves in 3D. Rose-shaped curves with four petals were generated at different shape parameters. The data points are defined in 3D as follows:

For the first petal: $q_0 = (0, 0, 0)$, $q_1 = (2, 2, 1)$, $q_2 = (0, 3, 1)$, $q_3 = (0, 0, 0)$.

For the second petal: $q_4 = (0, 0, 0)$, $q_5 = (-2, 2, 1)$, $q_6 = (-3, 0, 1)$, $q_7 = (0, 0, 0)$.

For the third petal: $q_8 = (0, 0, 0)$, $q_9 = (-2, -2, 1)$, $q_{10} = (0, -3, 1)$, $q_{11} = (0, 0, 0)$.

For the fourth petal: $q_{12} = (0, 0, 0)$, $q_{13} = (2, -2, 1)$, $q_{14} = (3, 0, 1)$, $q_{15} = (0, 0, 0)$.

Figure 17$a$ shows the interpolated CHTB curve at $\beta = -1$, $\nu = 1$, $\gamma = 1$, and $\lambda = 0$. The red curves use uniform parametrization; the blue curves use centripetal parametrization, and the purple curves use chordal parametrization.

Figure 17$b$ depicts the interpolated CHTB curve at $\beta = -1$, $\nu = 0.5$, $\gamma = 1$, and $\lambda = 0$, using the same data point.

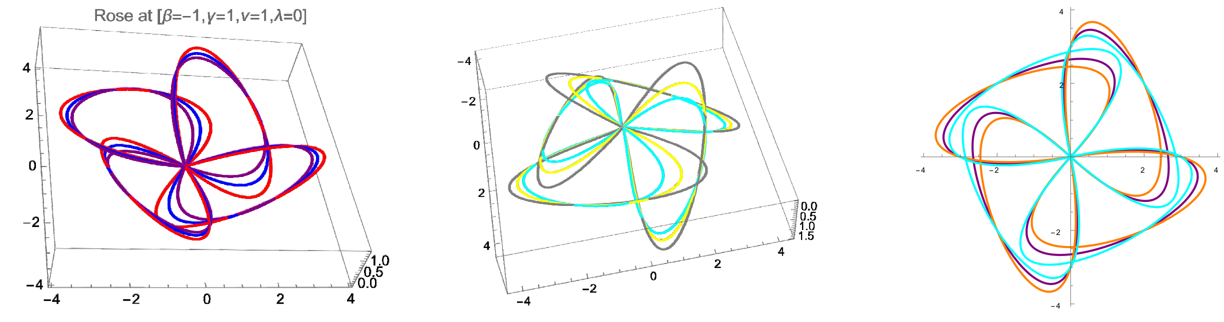


***a*** ***b*** ***c***

**Fig. 17.** Rose shape at shape parameters (***a***) $\beta = -1$, $\nu = 1$, $\gamma = 1$, and $\lambda = 0$, (***b***) $\beta = -1$, $\nu = 0.5$, $\gamma = 1$, and $\lambda = 0$, (***c***) $\beta = -1$, $\nu = 0.5$, $\gamma = 1$, and $\lambda = 0$.

When the same data points are used in 2D space to get the interpolated CHTB curve at $\beta = -1$, $\nu = 1$, $\gamma = 1$, and $\lambda = 0$, the flower pattern is shown in Figure 17$c$.

The present applications exemplify our methodology for space curve analysis. The black curves in the pictures correspond to the known or sketched portions, while the lacking section is predicted using the interpolated CHTB curve.

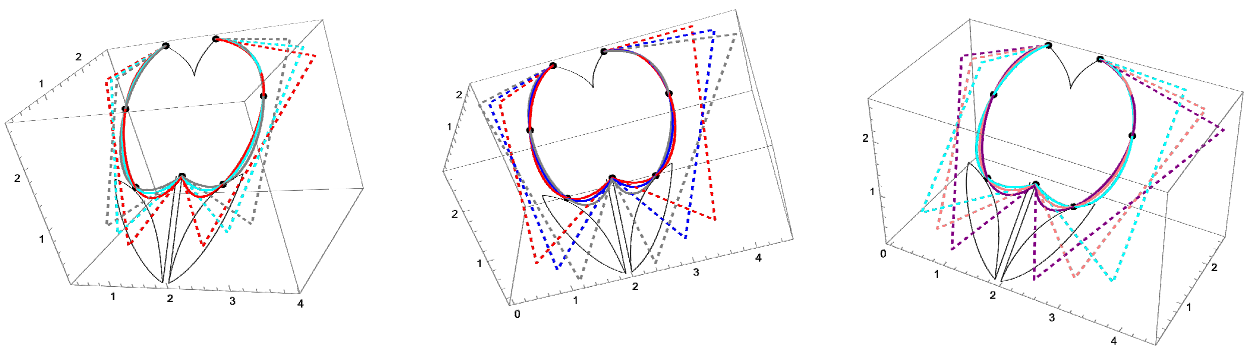

***a*** ***b*** ***c***

**Fig. 18.** Flower with three parametrization methods for space CHTB curve at (***a***) $\beta = 1$, $\nu = 1$, $\gamma = 1$, and $\lambda = 0$, (***b***) $\beta = 0$, $\nu = 0$, $\gamma = 0$, and $\lambda = 0$, (***c***) $\beta = -1$, $\nu = -1$, $\gamma = -1$, and $\lambda = 0$.

In Figures 18$a$, 18$b$, and 18$c$, the uniform, centripetal, and chordal parameterization methods were used to interpolate the space CHTB curve.

Figures 19$a$, 19$b$, and 19$c$ depict the computational modeling of cetaceans utilizing interpolated spatial CHTB curves constructed using three parametric approaches. The shape parameters used are: $\beta = \nu = \gamma = 1$, $\lambda = 0$, $\beta = \nu = \gamma = \lambda = 0$, and $\beta = \nu = \gamma = -1$, $\lambda = 0$, respectively.

A certain impact of the shape parameter is evident in the modelling of the figures.

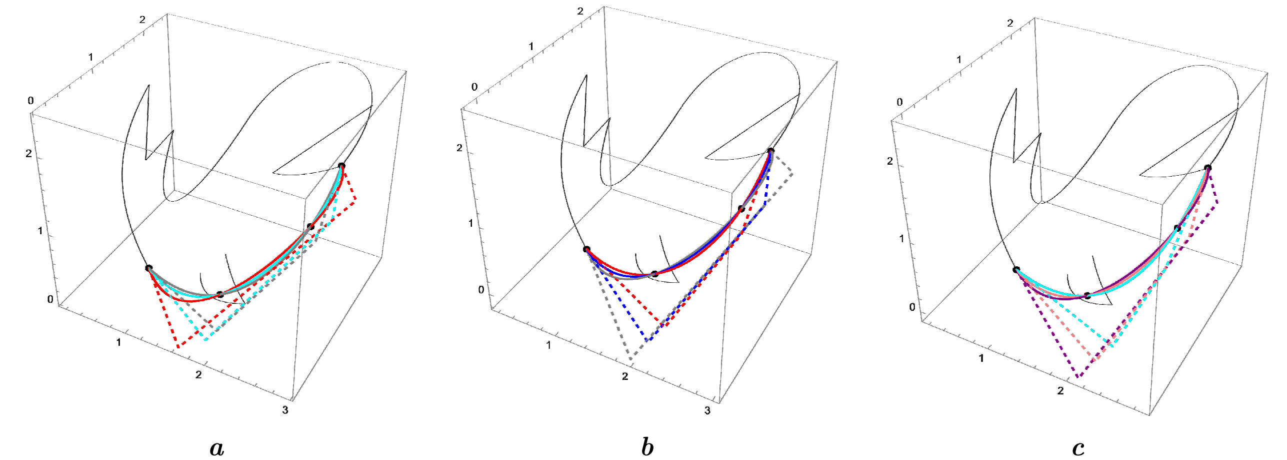


**Fig. 19.** Cetacean with three parametrization methods for space CHTB curve at (***a***) $\beta = 1$, $\nu = 1$, $\gamma = 1$, and $\lambda = 0$, (***b***) $\beta = 0$, $\nu = 0$, $\gamma = 0$, and $\lambda = 0$, (***c***) $\beta = -1$, $\nu = -1$, $\gamma = -1$, and $\lambda = 0$.

Figures 20$a$, 20$b$, and 20$c$ depict a rat modeled using interpolated CHTB curves, utilizing the three parametrization approaches for various shape parameters.

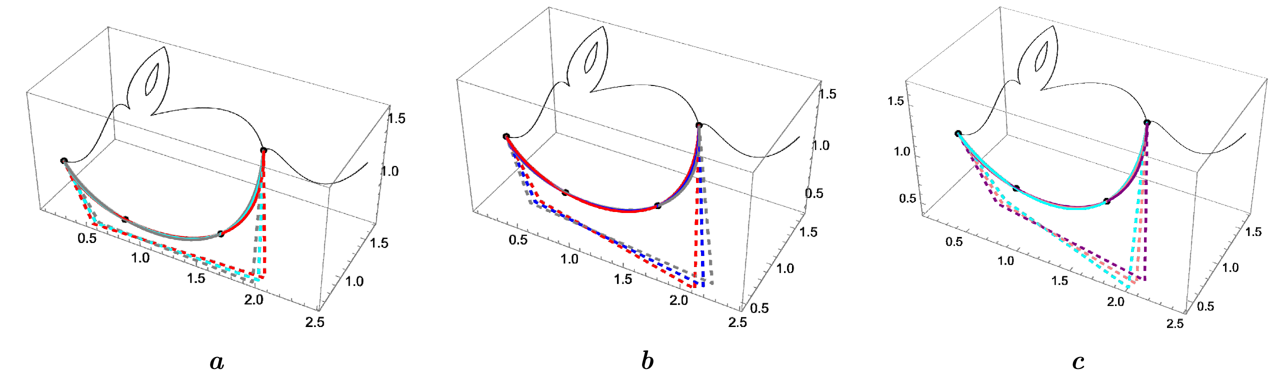


**Fig. 20.** Rat with three parametrization methods for space CHTB curve at (***a***) $\beta = 1$, $\nu = 1$, $\gamma = 1$, and $\lambda = 0$, (***b***) $\beta = 0$, $\nu = 0$, $\gamma = 0$, and $\lambda = 0$, (***c***) $\beta = -1$, $\nu = -1$, $\gamma = -1$, and $\lambda = 0$.

## 5. Conclusions

In this paper, the interpolation of GHTB curves is performed using the uniform, centripetal, and chordal parametrization methods. For comparison purposes, the curve for selected parameters $\beta = -1$, $\nu = 1$, $\gamma = 1$, and $\gamma = 0$ were shown, alongside the curves where the parameters are $\beta = 1$, $\nu = -1$, $\gamma = 1$, and $\lambda = 0$, in both 2D and 3D Euclidean spaces. In principle, designers can choose suitable parameters for their design. The choice of the parametrization method and its impact on curvature and torsion will be influenced by both the parameters and the characteristics of the data. Experimentation and adjustment of data points or parameters are often necessary to determine the most suitable curve.

This raises an important question for our future research. Given that parameters can be selected arbitrarily to interpolate the specified data points, it is of interest to identify the optimal parameterization that will render the constructed curve aesthetically pleasing.

### Acknowledgment

This research is supported by the Ministry of Higher Education Malaysia through the Fundamental Research Grant Scheme (FRGS/1/2021/STG06/USM/02/6).

[1] Gerald F. A History of Curves and Surfaces in CAGD. Handbook of Computer Aided Geometric Design. 1–21 (2002).

[2] Ammad M., Ramli A. Cubic B-Spline Curve Interpolation with Arbitrary Derivatives on its Data Points. 2019 23rd International Conference in Information Visualization – Part II. 156–159 (2019).

[3] Harada K., Nakamae E. Application of the Bézier curve to data interpolation. Computer-Aided Design. **14** (1), 55–59 (1982).

[4] Farouki R. T., Neff C. A. Hermite interpolation by Pythagorean hodograph quintics. Mathematics of Computation. **64**, 1589–1609 (1995).

[5] Pelosi F., Farouki R. T., Manni C., Sestini A. Geometric Hermite Interpolation by spatial Pythagorean-hodograph cubics. Advances in computational Mathematics. **22**, 325–352 (2005).

[6] Walton D. J., Meek D. S. $G^1$ interpolation with a single Cornu spiral segment. Journal of Computational and Applied Mathematics. **223** (1), 86–96 (2009).

[7] Okaniwa S., Nasri A., Lin H., Abbas A., Kineri Y., Maekawa T. Uniform B-Spline Curve Interpolation with Prescribed Tangent and Curvature Vectors. IEEE Transactions on Visualization and Computer Graphics. **18** (9), 1474–1487 (2012).

[8] Said H., Abdellah L., Danou B., Lotfi M. Hermite interpolation by piecewise cubic trigonometric spline with shape parameters. Proceedings of the 1st International Conference of Computer Science and Renewable Energies ICCSRE. **1**, 277–283 (2018).

[9] Yang X. Geometric Hermite interpolation by logarithmic arc splines. Computer Aided Geometric Design. **31** (9), 701–711 (2009).

[10] Yang J., Ning T., Shen Y. Planar $G^3$ Hermite interpolation by quintic Bezier curves. The Visual Computer. **38**, 12 4319–4328 (2022).

[11] Balta C., Öztürk S., Kuncan M., Kandilli I. Dynamic centripetal parametrization method for B-spline curve interpolations. IEEE Access. **8**, 589–598 (2020).

[12] Mohd Syakir S., Ramli A. Bezier curve interpolation on road map by uniform, chordal, and centripetal parametrization. AIP Conference Proceedings. **1974** (1), 020087 (2018).

[13] Muhammad S., Ramli A. Cubic B-Spline Curve Interpolation with Arbitrary Derivatives on Its Data Points. 2019 23rd International Conference in Information Visualization – Part II. 156–159 (2018).

[14] Wen-tao W., Guo-zhao W. Bézier curves with shape parameter. Journal of Zhejiang University – SCIENCE A. **6**, 497–501 (2005).

[15] Misro M. Y., Ramli A., Ali J. M. Quintic Trigonometric Bézier Curve with Two Shape Parameters. Sains Malaysia. **46** (5), 825–831 (2017).

[16] Han X. Cubic trigonometric polynomial curves with a shape parameter. Computer Aided Geometric Design. **21** (6), 535–548 (2004).

[17] BiBi S., Abbas M., Miura K. T., Misro Md Y. Geometric modelling of novel generalized hybrid trigonometric Bézier-like curve with shape parameters and its applications. Mathematics. **8** (6), 967 (2020).

[18] Ammad M., Misro Md Y., Ramli A. A novel generalized trigonometric Bézier curve: Properties, continuity conditions and applications to the curve modeling. Mathematics and Computers in Simulation. **194**, 744–763 (2022).

[19] Maqsood S., Abbas M., Miura K. T., Majeed A., Iqbal A. Geometric modeling and applications of generalized blended trigonometric Bézier curves with shape parameters. Advances in Difference Equations. **2020**, 550 (2020).

[20] Bashir U., Abbas M., Ali J. Md. The $G^2$ and $C^2$ rational quadratic trigonometric Bézier curve with two shape parameters with applications. Applied Mathematics and Computation. **219** (20), 10183–10197 (2013).

[21] Usman M., Abbas M., Miura K. T. Some Engineering Applications of New Trigonometric Cubic Bezier-Like Curves to Free-Form Complex Curve Modeling. Journal of Advanced Mechanical Design, Systems, and Manufacturing. **14** (4), 19-00420 (2020).

[22] Naseer S., Abbas M., Emadifar H., Bi Bi S., Nazir T., Shah Z. H. A Class of Sextic Trigonometric Bézier Curve with Two Shape Parameters. Journal of Mathematics. **2021**, 9989810 (2021).

[23] BiBi S., Misro Md., Abbas M. Smooth path planning via cubic GHT-Bézier spiral curves based on shortest distance, bending energy and curvature variation energy. AIMS Mathematics. **6** (8), 8625–8641 (2021).

[24] Ameer M., Abbas M., Shafiq M., Nazir T., Birhanu A. Generalized Bézier-like model and its applications to curve and surface modeling. PLoS ONE. **19** (6), e0303340 (2024).

[25] Bibi S., Abbas M., Misro M. Y., Hu G. A novel approach of hybrid trigonometric Bézier curve to the modeling of symmetric revolutionary curves and symmetric rotation surfaces. IEEE Access. **7**, 165779–165792 (2019).

## Гібридна тригонометрична інтерполяція Безьє з рівномірною, хордовою та доцентровою параметризацією у 3-вимірному евклідовому просторі та її застосування

Мохамед Д., Рамлі А. Л. А.

*Школа математичних наук, Малайзійський науковий університет (USM), 11800 Пулау Пінанг, Малайзія*

Інтерполяція в тригонометричних кривих Безьє полягає в побудові кривої, що плавно проходить через заданий набір контрольних точок. У цій роботі інтерполяція точок даних виконується за допомогою загальної гібридної тригонометричної кривої Безьє (GHTB). Ця крива містить чотири вільні параметри, що забезпечує гнучкість у її побудові. Визначення контрольних точок на GHTB кривій, виходячи з певної степені, дозволяє інтерполювати криву, яка проходить через задані точки. До кривих GHTB застосовуються методи рівномірної, доцентрової та хордової параметризації. У статті обговорюються ці три методи параметризації кривої GHTB: рівномірна, доцентрова та хордова. Згодом ці методи параметризації демонструються з використанням наборів точок даних як у 2-вимірному, так і в 3-вимірному евклідовому просторі. Досліджуються кривина та кручення параметризованих кривих для різних значень вільних параметрів у GHTB кривій.

**Ключові слова:** *загальна гібридна тригонометрична крива Безьє; рівномірна параметризація; доцентрова параметризація; кручення.*